Rev. Roum. Sci. Techn.– Électrotechn. et Énerg.
Vol. **70**, *3*, pp. 403–400, Bucarest, 2025

EFFECT OF SUPERIMPOSED DC AND AC ELECTRIC FIELDS ON WATER VAPOR CONDENSATION IN A CORONA REACTOR

ALEX-STEFAN VASILIU[1], LAURENTIU MARIUS DUMITRAN[1]

Keywords: Humidity control; Corona discharge reactor; DC and AC electric fields.

Humidity control in various rooms or installations, whether small or large, is a constant concern. Heat exchangers are generally used whose temperature is maintained below the dew point. Thus, water vapor condenses on the surface of these cooled elements, and the water can be extracted in liquid form. Energy efficiency and effective control of these installations are two critical aspects that are of constant interest in practical applications. This paper presents an experimental study on the condensation efficiency of water vapor in a cylindrical reactor with controlled temperature and corona discharges obtained with a wire electrode positioned on its central axis and supplied with a continuous positive or negative electric voltage. Thus, as a first step, the influence of corona discharges and the DC electric field on the efficiency of water vapor condensation is investigated. Secondly, the experimental study also explores the impact of an AC field superimposed over the DC field corresponding to the corona discharge. The obtained results indicate that the application of the AC electric field superimposed over the DC corona field significantly improves the condensation efficiency of water vapor.

1. INTRODUCTION

Corona discharges represent a regime of non-homogeneous discharge that occurs around conductors or metallic electrodes with a small radius of curvature when the electric field strength exceeds the ionization threshold of air but remains below the level necessary for a complete disruptive discharge. This phenomenon generates a weakly ionized plasma and charged species (ions, electrons, and excited molecules), which constitute a spatial electric charge existing in a nonuniform electric field. The specific phenomena of corona discharge are complex, but in simplistic terms, neglecting the ionization zone located near the electrode surface where the discharge occurs, they can be considered as representing a unipolar injection of ions that move along the electric field lines and generate the corresponding electric current of the discharge [1,2].

Consulting the extensive literature in the field of applied electrostatics, it can be observed that corona discharge has been extensively utilized in numerous applications. In electrostatic air filtration [1,3,4], they are used to charge suspended solid or liquid particles, which are subsequently collected on grounded electrodes under the influence of the electric field. This method is essential in industrial facilities for reducing fine particle emissions. Also, in the field of material recycling and granular mixtures (metal–polymer) processing, electric fields generated by corona discharges allow for the separation of solid components based on their electrostatic properties (electric conductivity and permittivity), being applied in plastic material recovery, the mining industry, and waste sorting [5–7]. Another notable field is electrostatic painting, where paint or powder particles are electrically charged and attracted to the surface of the workpiece, resulting in uniform coatings, increased adhesion, and reduced material waste [8,9].

The interaction between electric fields and phase change processes, especially the condensation of water vapor, has become a significant topic of interest in recent decades due to its implications in fields such as gas treatment, heat transfer, moisture capture, and the optimization of energy processes. Electric fields can significantly influence the nucleation and growth processes of condensation droplets through dielectrophoretic forces and by altering the charge distribution in the vicinity of cold surfaces. Thus, either the acceleration of the condensation process or better control of the morphology of the formed water film can be achieved.

Numerous studies have investigated the influence of static electric fields (DC) on condensation, particularly in parallel plate configurations or in systems with more complex shapes of the electrodes [10-13]. Among these, the studies conducted by Reznikov et al. [9, 10] have demonstrated that the application of an electric field can reduce the energy required for the formation of condensation nuclei and can accelerate the process of droplet coalescence, leading to a faster and more controlled condensation of water vapor. Other research has highlighted the influence of the size and shape of the electrodes, as well as the field strength on the distribution of the condensate [14, 15].

In contrast, the effects of alternating fields (AC) or even DC–AC superimposed fields, especially in the presence of an ionized medium such as that generated by corona discharges, remain significantly less explored. Fields of this type can induce additional instabilities in the gas boundary layer, influencing the ion mobility and modifying the electroaerodynamic behaviour of vapours, with direct implications for condensation mechanisms. Additionally, the presence of a corona discharge generates an environment with a complex distribution of ions and electrons, which can lead to changes in local field, relative humidity, and temperature—factors that influence condensation in a nontrivial manner.

In this context, the present work aims to investigate the influence of the superposition of direct electric field (DC) and alternating electric field (AC) on the process of water vapor condensation in a corona discharge reactor. Thus, the paper aims to evaluate the combined effect of DC–AC fields on the condensation rate and to examine the influence of electrical parameters (voltage level, voltage polarity, AC voltage frequency, and air velocity) on condensation efficiency. Through these objectives, the study contributes to the understanding of the mechanisms by which electric fields can influence phase change in ionized gases, with potential applications in the development of advanced humidity control systems, physicochemical separation, and energy recovery.

[1] Laboratory of Electrotechnical Materials, Faculty of Electrical Engineering, National University of Science and Technology Politehnica Bucharest, Romania. E-mails: alex_stefan.vasiliu@upb.ro, laurentiu.dumitran@upb.ro.

DOI: 10.59277/RRST-EE.2025.70.3.20

2. WATER VAPOR CONDENSATION IN ELECTRIC FIELDS

The phenomena that take place in simple phase change heat exchangers without any boost created by an electric field or space charge are directly related to condensation, which can be either heterogeneous (caused by contact between a liquid or solid surface) or homogenous (caused by the formation of atomic/molecular clusters such as water droplets). Numerous studies have examined the basic issue of condensation [16, 17]. The vapor pressure is one of the main factors that determine the rate of condensation (which refers to the number of water molecules that transition from the gas phase to the liquid phase every second). Thermodynamics and kinetics of nucleation indicate that the rate of condensation increases as the water vapor pressure, p, rises [17]. Therefore, if the water droplets and vapor are in balance, the saturation level of humid air is reached [17]. The condensation of water vapor begins with the formation of liquid phase embryos – microscopic droplets. Gibbs' theory defines the energy required for a droplet to grow or evaporate. Free Gibbs energy associated with the nucleation process is given by [17]:

$$\Delta G(r)=4\pi r^2\sigma-\frac{4}{3}\pi r^3\Delta g_v, \tag{1}$$

where r [m] is the radius of the incipient water droplet, σ [N/m] is the surface tension, and $\Delta g_v=(kT/v_l)\cdot lnS$ is the free Gibbs energy per unit volume with $S = p/p_{sat}$ in which p_{sat} [Pa] is the saturation pressure, v_l [m^3/mol] is the molar volume of the liquid phase, and $k = 1.38\cdot10^{-23}$ J/K is the Boltzmann constant. Thus, the critical radius (for which the probabilities of condensation and evaporation are equal and the droplet as a cluster becomes stable) can be expressed by the relationships [17]:

$$r_c=\frac{2\sigma v_l}{kT\cdot\ln S} \tag{2}$$

which indicates that if S [m^2] increases, the critical radius of the droplet decreases, and the nucleation process is favored.

In a simplified manner, the nucleation rate ϕ [nuclei/m·s] of the vapors can be written as [17]:

$$\phi(p)=A(r_c)\cdot\frac{p\cdot c}{T^{1/2}}\cdot\exp\left(-\frac{\Delta G}{kT}\right) \tag{3}$$

where c is the water vapor molecule concentration, T [K] is the temperature, and $A(r_c)$ is a factor depending on the critical radius r_c of the droplet and thermodynamic conditions. Therefore, equation (3) establishes the mathematical relationship between the condensation rate, on one hand, and the vapor pressure and water molecule concentration, on the other hand. It is also observed that if the value of the Gibbs free energy decreases, the nucleation rate increases, which practically means that the condensation phenomenon intensifies.

Previous studies [10-13] demonstrate that the presence of charged particles in the carrier air significantly affects the condensation rate of water vapor. An external electric field $\vec{E}$ (E [V/m]) modifies the energy balance in the Gibbs theory by an additional energy associated with the droplet's polarizability. In a simple case of a uniform electric field, the added electrostatic energy is expressed as [10, 20, 21]:

$$\Delta G_E=-\frac{1}{2}\varepsilon_0\varepsilon_r\alpha E^2 \tag{4}$$

and the total free Gibbs energy becomes:

$$\Delta G(r)=4\pi r^2\sigma-\frac{4}{3}\pi r^3\Delta g_v-\frac{1}{2}\varepsilon_0\varepsilon_r\alpha E^2. \tag{5}$$

In (4) and (5), the quantity $\varepsilon_0=8.85\cdot10^{-12}$ F/m is the vacuum permittivity, ε_r is the relative permittivity of the water, and α is the polarizability of the water droplet, which, for a spherical droplet, can be expressed as [20]:

$$\alpha=4\pi\varepsilon_0 r^3\frac{\varepsilon_r-1}{\varepsilon_r+2}. \tag{6}$$

Therefore, the electric field contributes to the reduction of Gibbs free energy and, consequently, to the decrease of the critical effective nucleation radius [20, 21]

$$r_c^{eff}=\frac{2\sigma}{\Delta g_v+\Delta g_E}, \tag{7}$$

where the term Δg_E is the density of the electrostatic field energy. This also explains why the electric field favors the nucleation and growth of condensed droplets, accelerating the phase transition.

Let's now consider the situation of a phase change heat exchanger with a non-uniform spatial charge consisting of positive and/or negative ions (for example, generated through a corona discharge). First of all, its presence causes a change in the distribution of the electric field compared to the previous case, where it was considered uniform. As presented in [12, 13], in the case of a wire-cylinder geometry reactor, with the central wire serving as the corona electrode and supplied with a negative DC high voltage, the problem can be analyzed in a simplified manner by assuming the wire surface as a monopolar source of negative ions. The ions generated by the corona discharge are subjected to electrostatic forces due to the electric field and move along the field lines, giving rise to the corona current. Neglecting the diffusion phenomenon, the expression for the electric current density (J [A/m^2]) passing through the space between the wire electrode and the inner surface of the grounded cylinder is:

$$\vec{J}=\rho_i\mu_i\vec{E}, \tag{8}$$

where ρ_i is the ionic space density and μ_i [m^2/V·s] is the mobility of ions. For small water droplets (with a diameter of the order of 10^{-6} m), based on the diffusion-electric field charging model [22], the expression of acquired electric charge q [C] is:

$$q=4\pi\varepsilon_0\varepsilon_r r^2E, \tag{9}$$

which leads to an increase in total free Gibbs with [20]

$$\Delta G_q=\frac{q^2}{8\pi\varepsilon_0 r}. \tag{10}$$

Therefore, the electrical charging of particles and, consequently, the increase in Gibbs free energy led to a slight decrease in the nucleation rate. However, ions act as heterogeneous nucleation centers around which nucleation clusters can form, thus favoring the condensation phenomenon.

Another important aspect concerns the electroaerodynamic phenomena (EAD) induced by corona discharge. As presented in [12, 23], in general terms, these

phenomena are known as ionic wind and consist of air movement resulting from ions being dragged by an electric field. This movement unfolds radially in the case of the considered wire-cylinder configuration. Its interaction with the main airflow passing through the cylindrical reactor gives rise to a complicated turbulent flow. These phenomena have major effects on the condensation process by reducing the diffusion layer, increasing vapor transport towards the cold zone (cylinder surface), modifying the local distribution of temperature and relative humidity, and also inducing convection currents that favor droplet coalescence and drainage.

The last point discussed in this section concerns the case where a sinusoidal alternating field is superimposed over the DC field that produces corona discharge. The total field becomes:

$$E(t)=E_{DC}+E_{AC}\sin\omega t, \tag{11}$$

which leads to variable Gibbs energy

$$\Delta G_{E(t)}=-\frac{1}{2}\varepsilon_0\varepsilon_r\alpha[E_{DC}+E_{AC}\sin\omega t]^2. \tag{12}$$

Thus, at frequencies lower than the order of kHz, ions can respond to the alternating field $E_{AC}(t)$. Therefore, the superposition of the alternating field causes a change in the spatial charge distribution (with screening/displacement effects), the appearance of oscillating electric forces on the ions and polar water molecules, which makes nucleation dependent on the phase of the electric field.

3. EXPERIMENTAL SET-UP AND METHOD

The experimental study was conducted using a temperature-controlled stainless-steel wire-cylinder reactor. Figure 1 presents a schematic view of the reactor. Figure 2 shows an image of the reactor with the central corona wire made of tungsten and having a diameter of d_f = 0.075 mm. The metallic cylinder has an inner diameter of 46 mm, and the total active length of the reactor is 240 mm.

The corona reactor is integrated into a complex system, schematically represented in Fig. 3. As can be seen, the collector cylinder temperature is regulated using a closed system within which glycol is circulated with the help of an adjustable electric pump. The cooling elements are Peltier-type and can provide a minimum temperature of approximately 4 °C for the cooling system. The humid air

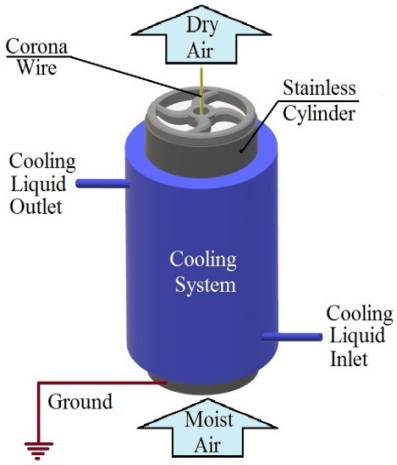

Fig.1 – Schematic view of the wire-cylinder condenser.

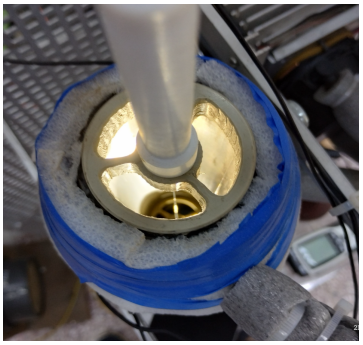

Fig.2 – Top view of the wire-cylinder condenser.

treated inside the reactor has a humidity of over 96% and is obtained using a system composed of an atomizer and a chamber with a volume of approximately 0.6 m^3. The humid air circulates through the reactor via polyethylene pipes connected to the lower and upper parts of the active stainless-steel cylinder, respectively, and a variable-speed turbine mounted on the exhaust pipe at approximately 0.8 m. The average air velocity can be adjusted within the range of 0.05 – 3.2 m/s and is measured at a distance of 30 cm from the reactor outlet using a hot-wire anemometer. Temperature and humidity are continuously measured both at the reactor inlet and outlet. Additionally, the corona current is monitored throughout the experiments using a microammeter connected between the stainless-steel cylinder and ground.

To determine the condensation efficiency, ΔRH [%] (calculated as the difference between RH_{inlet}[%] and RH_{outlet}[%]), the values of humidity and temperature of the treated air were continuously monitored both at the reactor inlet and outlet. Tests conducted beforehand in a closed chamber that ensured moisture and temperature regulation showed that the two measuring devices used provided similar readings within the humidity range of RH 60-94%. Additionally, the hot-wire anemometer used to determine the average air velocity value in the system was calibrated each time before an experiment.

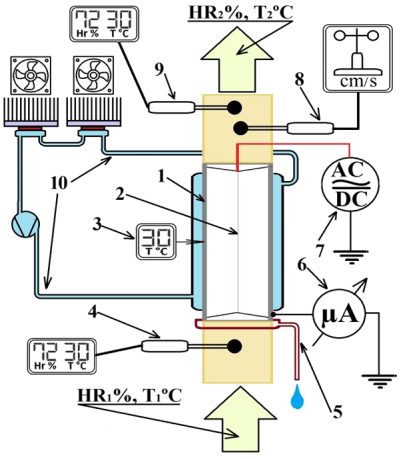

Fig.3 – Schematic view of the experimental set-up: 1-cold cylinder of the condensation reactor, 2 - corona wire, 3 – temperature measurement system of the reactor cylinder, 4 – humidity/temperature measuring device probe at the inlet of the reactor, 5 – collected water drainage system, 6 – microammeter for corona current measurement, 7 – adjustable power supply for DC and AC voltage, 8 – anemometer probe, 9 – humidity/temperature measuring device probe at the outlet of the reactor and, 10 – cooling system.

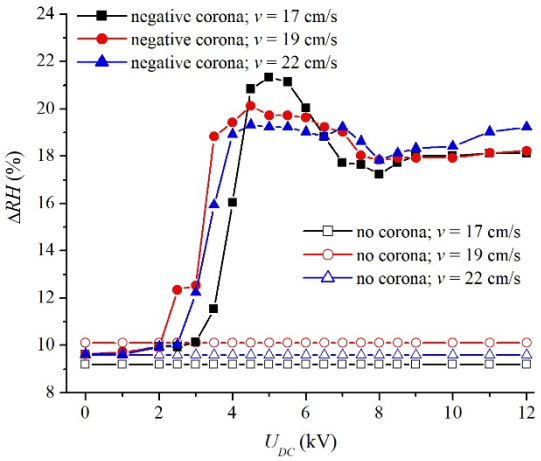

Fig. 4 – The operating characteristics of the corona reactor for negative DC voltage and three air flow velocities v of 17 cm/s, 19 cm/s, and 22 cm/s.

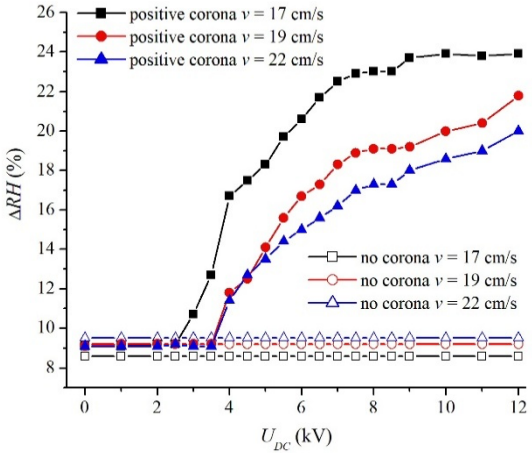

Fig. 5. – The operating characteristics of the corona reactor for positive DC voltage and three air flow velocities v of 17 cm/s, 19 cm/s, and 22 cm/s.

The experiments were conducted in a room with a mean temperature of 22°C and a relative humidity of approximately 62%. Conducting an experiment involved going through the stages as detailed below. Thus, the cooling system and the air circulation turbine, which draws atmospheric air (unsaturated with water vapor) into the system, are started initially, and the temperature is allowed to stabilize in the cold cylinder. The time required to reach the dew point and maintain it is between 35 and 45 minutes. By adjusting the turbine speed, the average air velocity through the installation is regulated, and its value is measured using the anemometer. Next, the air saturation system with water vapor is activated, and the desired humidity at the entrance to the condensation reactor is awaited. Depending on the required humidity level, the mixing valve is adjusted, which allows the humidified air from the atomizer chamber to be supplemented with air from the surrounding environment. The values of the humidity and temperature were recorded at the reactor inlet and outlet.

To obtain the reactor's operating characteristic, namely the variation curve $\Delta RH(U_{DC})$, high DC voltage is applied to the corona electrode, and its value is increased. For determinations where an alternating voltage $U_{AC}(t)$ is applied over the continuous voltage, the latter is applied before the continuous one. In these circumstances, there is an initial determination at the beginning that reflects only the effect of $U_{AC}(t)$ voltage, which is then followed by the simultaneous superposition of the alternating and direct voltages. The effective values of the alternating voltage applied in the experiments were 2.5 kV and 5 kV, respectively.

Also, experimental measurements are initially performed by increasing U_{DC} value from zero, in 1 kV increments, until the maximum value of 12 kV is reached, and then while the DC voltage is gradually decreased back to zero. At the end of the measurements, when the voltage applied to the corona wire is stopped, a new determination of the static humidity and temperature is made at the inlet and outlet of the reactor, respectively. Based on the humidity values measured at the reactor inlet and outlet, respectively, at the beginning of the experiments (without an electric field) and at the end (also without an electric field), intrinsic condensation attributed solely to the cooled cylinder is obtained, as referred to in this study.

Additionally, the differences obtained between the inlet and outlet humidity of the condensation reactor during the application of the electric field are averaged over the two directions of the determination (increasing and decreasing U_{DC}, respectively), which allows for obtaining the reactor's operating characteristic. The average duration of such an experiment is approximately 3 hours.

4. EXPERIMENTAL RESULTS

Several experimental results were obtained using the method presented in the previous section. Some of these will be presented and analyzed below. Thus, in the first stage, the operating characteristic of the corona reactor was determined for several values of the average air velocity, when the ionizing wire was supplied exclusively with DC positive and negative voltage (U_{DC}) – Figs. 4 and 5. Firstly, it can be observed that in the presence of corona discharges ($U_{DC} > \sim 3$ kV), ΔRH increases significantly. If in the case of negative DC voltage, the maximum condensation efficiency is obtained around -5 kV, in the case of positive voltage, ΔRH increases with the U_{DC}, recording the highest values +11÷12 kV. Also, Fig. 4 indicates that for negative corona voltage and $U_{DC} > 6$ kV, ΔRH decreases, which, compared to the results obtained for positive corona, represents a significant difference. Most likely, this can be attributed to the fact that, at the same applied voltage, negative corona discharge causes a stronger ionization of the air compared to positive corona discharge [2] (the ionic space charge created by negative corona discharge has a higher volume density than that produced by positive corona discharge). Consequently, in the case of a negative corona, there is higher electrical charging of the water microdroplets, which, according to (10), leads to a decrease in the nucleation rate. On the other hand, the presented results clearly show that as the air flow velocity increases from 17 cm/s to 22 cm/s, the condensation efficiency decreases.

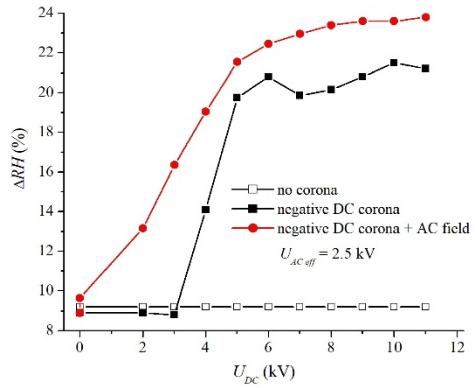

Fig. 6 – The operating characteristics of the corona reactor for negative DC corona and superimposed AC electric field: v = 17 cm/s, $U_{AC\,eff}$ = 2.5 kV, and f =19 kHz.

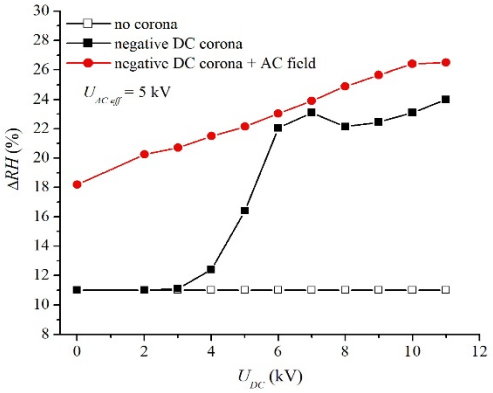

Fig. 7 – The operating characteristics of the corona reactor for negative DC corona and superimposed AC electric field: v = 17 cm/s, $U_{AC\,eff}$ = 5 kV, and f =19 kHz.

Figures 6 and 7 present the operating characteristics of the reactor in the presence of a negative corona discharge and an alternating electric field produced by superimposing an alternating voltage with an effective value of 2.5 kV and, respectively, 5 kV and a frequency of f = 19 kHz. It can be observed that the presence of the alternating electric field leads to a significant increase in condensation efficiency even for low values of U_{DC} voltage, below the threshold value at which the corona discharge is initiated (~3 kV). For example, for U_{DC} = 6 kV, applying the alternating voltage U_{AC} = 2.5 kV results in a 9.5% increase in ΔRH,

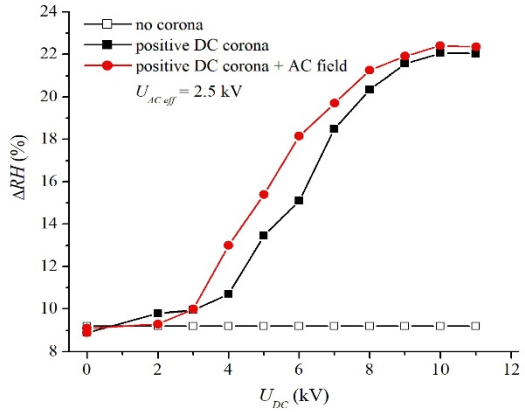

Fig. 8 – The operating characteristics of the corona reactor for positive DC corona and superimposed AC electric field: v = 17 cm/s, $U_{AC\,eff}$ = 2.5 kV, and f =19 kHz.

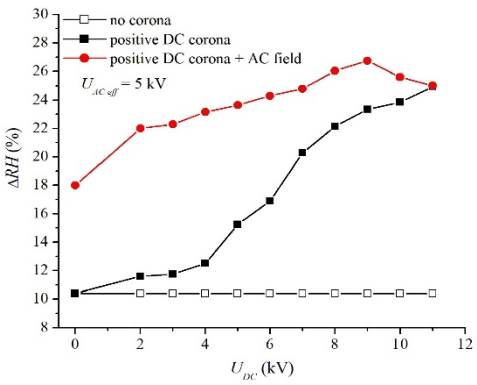

Fig. – The operating characteristics of the corona reactor for positive DC corona and superimposed AC electric field: v = 17 cm/s, $U_{AC\,eff}$ = 5 kV, and f =19 kHz.

while for U_{DC} = 8 kV, the increase is approximately 14.7%. In the case where U_{AC} = 5 kV, the operating characteristic changes substantially, showing significant increases and even doubling the ΔRH value in its first part. This time, for U_{DC} = 8 kV, the presence of alternating field leads to an increase in ΔRH by over 13.6%.

Figures 8 and 9 present the operating characteristics for positive corona discharge and superimposed alternating electric field, under the same conditions as above. Substantial changes can be observed for U_{AC} = 5 kV, when ΔRH shows very high increases. For example, at U_{DC} = 6 kV, ΔRH increases by over 41%, while for U_{DC} = 8 kV, the increase is about 16%.

Figure 10 shows the variation of ΔRH as a function of the frequency of the applied alternating voltage. Thus, even for a relatively narrow range of frequencies imposed by the capability of the power source, a clear trend of increasing condensation rate is observed if f increases from 17.5 kHz to 26 kHz. This indicates that the efficiency of such a reactor can still be improved by identifying those frequency values that most favorably influence the nucleation rate. A special mention refers to the value of the DC voltage applied to the corona wire, which, in the case of the results presented in Fig. 10, is 8 kV and, respectively, 8.25 kV. The experiments conducted in this study have shown that increasing the applied voltage beyond these values can, in certain situations, lead to effects that alter the condensation process. Among these, the most important are the Joule effect associated with corona electric current and, sometimes, electrical discharges that occur on wet surfaces.

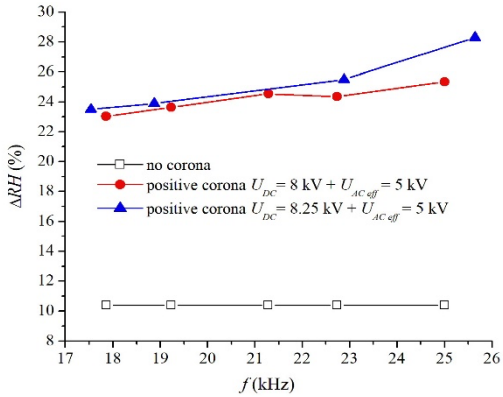

Fig. 10 – Variation of condensation efficiency as a function of alternating voltage frequency for positive corona (U_{DC} = 8 kV and 8.25 kV), v = 17 cm/s and $U_{AC\,eff}$ = 5 kV.

5. CONCLUSION

The present study highlights the influence of static and time-varying electric fields on the condensation process of water vapor in a wire-cylinder type corona discharge reactor. Based on the above experimental results, some critical observations can be synthesized. Firstly, it is observed that corona discharges lead to a significant increase in condensation efficiency. This increase is more pronounced when applying a positive DC voltage, for which the maximum efficiency was observed at values of 11 to 12 kV. In the case of negative discharges, optimal efficiency was achieved at a value of approximately 5 kV, followed by a decrease for higher values, most likely due to the electric charge acquired by the microdroplets of water. The superposition of an alternating electric field leads to a considerable improvement in the condensation rate. It has been observed that, for moderate values of AC voltage (2.5 kV and 5 kV at frequencies of ~19 kHz), an increase in ΔRH of up to 41% can be achieved, depending on the polarity and amplitude of the applied DC voltage. The effect is more pronounced in a positive discharge regime superimposed with an alternating field. Moreover, the effect of the alternating field remains relevant even in the absence of corona discharges, suggesting that additional mechanisms, such as droplet polarization and instabilities induced by oscillating EAD forces, contribute to promoting condensation.

The increase in the frequency of the applied alternating voltage also leads to a clear increase in the condensation rate, suggesting the existence of a frequency-sensitive dependence of the nucleation process. This result opens the way to explore further optimization by adjusting the frequency of the applied alternating voltage.

Generally, the presented results suggest that the combined use of continuous and alternating electric fields in a corona reactor represents a viable solution for intensifying condensation processes, especially in high-humidity regimes or controlled airflows. In this context, a future direction for research is the optimization of electrical parameters (amplitude, frequency, time-variable voltage waveform) in correlation with reactor geometry and environmental conditions (temperature, pressure, air flow rate).

Additionally, a more detailed investigation of electroaerodynamic effects and phenomena associated with space charge near collection surfaces is necessary to understand better the mechanisms by which droplet nucleation and coalescence are dynamically influenced.

Finally, the application of these principles in scalable devices for industrial applications — such as air dehumidification, water recovery from exhaust gases, or environmental control in enclosed spaces — represents a promising practical direction, with potential impact on energy efficiency and sustainability.

CREDIT AUTHORSHIP CONTRIBUTION STATEMENT

Alex-Stefan Vasiliu: Experimental set-up design, data collecting, methodology conceptualization, primary data analysis.
Laurentiu Marius Dumitran: Analysis and verification of data consistency, manuscript review, and editing.

Received on 24 July 2025

REFERENCES

1. L.B Loeb, *Electrical Coronas - Their basic physical mechanisms*, University of California Press, pp. 15-266 (1965).
2. K.R. Parker, *Applied Electrostatic precipitation*, Chapman & Hall, pp. 25–88 (1997).
3. H.J. White, *Industrial electrostatic precipitation*, Wesley Publishing Company, Inc., (1963).
4. D. Blanchard D, L.M. Dumitran, P. Atten, *Electroaerodynamic secondary Flow in an electrostatic precipitator and its influence on transport of small diameter particles*, Proc. 8th International Conference on Electrostatic Precipitation, Birmingham, paper A1-4 (2001).
5. L.M. Dumitran, L.V.Badicu, M. Plopeanu, L. Dascalescu, *Efficiency of dual wire-cylinder electrodes used in electrostatic separators,* Revue Roumaine Des Sciences Techniques-Serie Electrotechnique Et Energetique, **55,** *2*, pp.171–180 (2010).
6. J. Bohm, *Electrostatic precipitators*. Elsevier, pp. 11–366 (1982).
7. O.C. Ralston, *Electrostatic separation of mixed granular materials*, Elsevier (1961).
8. G.H. Douma, J. van Turnhout, P.H. Ong, *A study of the electrostatic powder-coating process by charge and current measurements*, Inst. of Physics Conf. Ser**. 27**, pp. 188-201 (1975).
9. A. Catinean, L. Dascalescu, M. Lungu, L.M. Dumitran, A. Samuila, *Improving the recovery of copper from electric cable waste derived from automotive industry by corona-electrostatic separation*, Particulate Science and Technology, **39,** *4*, pp. 449–456 (2021).
10. M. Reznikov, M. Salazar, M. Rivera – Sustache, M. Lopez, *Electrically enhanced harvesting of water vapor from the air,* Proc. ESA Annual Meeting on Electrostatics, USA, pp. 1-6 (2015).
11. M. Salazar, K. Minakata, M. Reznikov, *Electrostatic enforcement of steam power plant*, IEEE IAS Annual Meeting, USA, pp. 1-5 (2016).
12. S.A. Vasiliu, L.C. Popescu, A. Stanescu, L.M. Dumitran, *Efficiency of water extraction in an electrostatic wire-cylinder system*, Int. Symposium on Fundamentals of Electrical Engineering ISFEE Bucharest, Romania (2023).
13. L.M. Dumitran, C.D. Oancea, G.E. Dumitran, *Experimental study of air dehumidification in an electrostatic wire-cylinder condenser,* 10th International Symposium on Advanced Topics in Electrical Engineering, Bucharest, Romania, pp. 440-433 (2017).
14. P. Birbarah, Z. Li, A. Pauls, N. Miljkovic, *A comprehensive model of electric-field-enhanced jumping-droplet condensation on superhydrophobic surface*s, Langmuir Journal, **31**, *28*, pp.7885–7896 (2015).
15. M.-K. Kim, H. Cha, N. Miljkovic, E.N. Wang, *Enhanced jumping droplet departure*, Langmuir Journal, **34**, *5,* pp. 2048–2058 (2018).
16. P.G. Debenedetti, *Metastable Liquids: Concepts and Principles*, Princeton University Press (1996).
17. H. Vehkamäki, *Classical Nucleation theory in multicomponent systems*, Springer (2006).
18. A.H. Biermann, *Homogeneous nucleation of water vapor in inert gas atmospheres*, Doctoral Dissertation, Missouri Univ. of. Science and Technology, USA (1971).
19. A.I. Rusanov, *Thermodynamic theory of nucleation on charged particles*, J. of Colloid and Interface Science, **68,** pp. 32-47 (1979).
20. V.B. Warshavsky, A.K. Shchekin, *The effects of external electric field in thermodynamics of formation of dielectric droplet*, Colloids and Surfaces A: Physicochemical and Engineering Aspects, **148,** *3*, pp. 283-290 (1999).
21. A.K. Shchekin, T.S. Podguzova, *The modified Thomson equation in the theory of heterogeneous vapor nucleation on charged solid particles,* Atmospheric Research, **101**, pp. 493-502 (2012).
22. M. Pauthenier, M. Moreau-Hanot, *La charge des particules sphériques dans un champ ionisé,* Journal de Physique et le Radium, **3,** pp. 590-613 (1932).
23. A. Niewulis, J. Podlinski, A. Berendt, J. Mizerazcyc, *Influence of electrode geometric arrangement on the operation of narrow circular electrostatic precipitator*, Int. J. of Plasma Environmental Science & Technology, **8,** *1*, pp. 60-71 (2014).